01 Jan 2018

Behavior of EB FRP Masonry Bond under Service Temperature

Zuhair Al-Aljaberi

John J. Myers
Missouri University of Science and Technology, jmyers@mst.edu

K. Chandrashekhara
Missouri University of Science and Technology, chandra@mst.edu

Recommended Citation

Z. Al-Aljaberi et al., "Behavior of EB FRP Masonry Bond under Service Temperature," *Advanced Materials Letters*, vol. 9, no. 11, pp. 753-759, VBRI Press, Jan 2018.

Behavior of EB FRP masonry bond under service temperature

Zuhair Al-Jaberi[1], John J. Myers[2]*, K. Chandrashekhara[3]

[1]*Graduate Research Student: Civil, Arch. and Envir. Engr, Missouri University of Science and Technology, Rolla, MO 65409, USA.*
[2]*Professor of Civil, Arch. and Envir. Engineering and Associate Dean, Missouri University of Science and Technology, Rolla, MO 65409, USA.*
[3]*Curators Distinguished Professor of Mechanical Engineering, Missouri University of Science and Technology, Rolla, MO 65409, USA.*

*Corresponding author

DOI: 10.5185/amlett.2018.2152
www.vbripress.com/aml

Abstract

The interest in advanced composites in repairing and strengthening infrastructure systems has considerably increased, especially as the application externally bonded (EB) fiber reinforced polymer (FRP) has become more well established. Previous research on bond behavior has focused on impact of durability by considering exposure to harsh environmental conditions and testing the specimens after exposure, rather than testing bond performance during exposure. The influence of directly applying temperature on bond behavior represents an open topic that needs to be investigated in more detail. This study is one of the first studies to investigate the bond behavior when the composite is subjected to tension force simultaneously with applying temperature. The temperatures considered in this study were at freezing, ambient, and high temperature, which are more representative of structural elements under field conditions. A total of 16 specimens were strengthened and tested under single-lap direct shear. The key parameters investigated include (a) the type of fiber [laminate carbon vs. wet layup glass] (b) the level of temperature applied on specimen, including ambient condition 21°C (70 °F), freeze condition -18 °C (0 °F) and hot weather 49 °C (120 °F), and (c) the exposure regime (direct exposure during loading process vs. loading after exposure). Most of the specimens were subjected to tension force simultaneously with applying temperature, and the other specimens were later tested after exposure to the heating and cooling cycles. These cycles are proposed to simulate 20 years of the typical in-situ weather conditions in the Central United States. The results showed that overall the EB strengthening systems exhibited good performance when subjected to cycles of heating and cooling prior to testing. High reduction of FRP-epoxy bond properties was up to 59% when exposed to high service temperatures. Different modes of failure were observed such as debonding at fiber-matrix interface and debonding due to shearing in laminate.

Keywords: Masonry, bond, FRP, temperature, durability.

Introduction

The wide use of externally bonded (EB) (including fiber reinforced polymer (FRP) and fiber reinforced cementitious matrix (FRCM)) in repairing and strengthening structural elements has considerably increased over the past two decades [1, 2]. The light weight, high strength and noncorrosive nature of advanced composite offer advantages over traditional techniques such as section enlargement and steel plate externally bonded [3]. The EB strengthening system consisted of fiber and epoxy resin. The epoxy resin influenced by the high and service temperature which is affected the bond performance. The effectiveness of the EB strengthening system is influenced significantly by the bond properties of the epoxy resin that used as adhesive material between the advanced composite and substrate interface. For the long- term durability evaluation, the glass transition temperature (T_g) is a useful tool used in evaluation process. Tatar and Hamilton [4] investigated the bond durability factor for externally bonded CFRP system. It was determined that bond durability factor for the wet layup system was equal to 0.6 and that there was not a significant difference between specimen subjected to 30 °C (86 °F) and 60 °C (140 °F) since both temperatures were less than T_g.

Masia et al. [5] characterized the bond behavior between the FRP and masonry unit based on pull-out test. The deterioration of FRP bond due to elevated temperature was investigated. This test also evaluated whether the bond deterioration is reversible or not. As a result of this study, the debonding of FRP subjected to sustained load initiated at temperatures close to the T_g of epoxy adhesive. The original bond strength was restored after cooling of heated specimens before applying load, and the mode of failure still the same compared with control specimens.

The effect of warm temperatures (less than 100 °C) on EB FRP strengthening system was investigated through short-term experimental work [6]. The experimental and analytical results showed that the adhesive softens at 40 °C (104 °F) and the slip increase that eventually causes a full debonding of the FRP when the temperature approximately reached the T_g of the adhesive.

A bond–slip relationship for EB-CFRP sheet under cyclic loading, was proposed [7]. The test results of this study and existing test results indicated that the slope of the ascending part of the bond–slip curve decreased with increase in the number of load cycles and the compressive strength of the substrate, but the slip corresponding to the maximum shear stress almost remained the same. The rate of reduction in the slope of the ascending part increased with an increase in the load level or the FRP/substrate width ratio, but the bond length had little effect on the rate.

The mechanical properties of glass FRP (GFRP) under different loads and thermal regimes were characterized [8]. The tensile strength and elastic modulus of wet lay-up GFRP reduced by 50% and 30% respectively. The bond strength of the system reduced by 60% at temperatures 15 °C below the T_g and approximately 90% at temperatures slightly above the T_g of its resin matrix.

The results of an experimental test to investigate the effect of elevated service temperature on EB FRP bonding were reported [9, 10]. The bond strength for CFRP sheet, GFRP sheet and CFRP laminate was reduced at 80 °C (176 °F) by 54%, 72%, and 25% respectively. The mode of failure changed from a cohesion to adhesion failure due to changing the temperature from 50 to 80 °C (122-176 °F). If the temperature was higher than T_g, the bond strength of the adhesive material reduced more than that of concrete and led to bond failure at the interface.

When a temperature close to the epoxy T_g occurred, the EB system lost bond strength due to phase change in material properties as reported by Cromwell et al. [11]. The durability and long-term performance of EB FRP-brick masonry bond under harsh environment was investigated by Maljaee et al. [12]. The specimens were exposed to cycles of temperature range between 10 °C and 50 °C (50 °F-122 °F) and constant relative humidity 90%. As a result of this study, the behavior of primer and epoxy adhesive changed from linear elastic to nonlinear behavior, this change was associated by reduction in both strength and stiffness.

Previous durability research on bond behavior has primarily focused on exposure to harsh environmental conditions and testing the specimens after exposure to the same conditions, which enables the adhesive material to reset before performing the bond test. However, this research focused on studying the bond behavior of EB system under direct application of different temperature (freeze, ambient, high temperature), which is more representative of structural elements in the field. This study will help to investigate for the first time the bond behavior when the EB system is subjected to tension force simultaneously with applying temperature.

The key parameters investigated in this study include (1) different types of fibers such as CFRP laminate vs. GFRP sheet, (2) different levels of temperature applied to the specimen such as at freezing temperature -18 °C (0 °F), at ambient temperature 21°C (70 °F), and at hot temperature 49 °C (120 °F). A total of sixteen specimens were strengthened and tested under single-lap direct shear. Twelve of these specimens were subjected to tension force simultaneously with applying temperature, and the remaining specimens were tested following exposure to the cycles of heating and cooling.

It is possible to use the results from these tests to develop an analytical model to represent the mechanical behavior of GFRP sheet or CFRP laminate under direct load and temperature, which is currently being developed by the authors.

Experimental study

Experimental program

Sixteen specimens were strengthened and tested under single-lap direct shear. Hollow concrete masonry units with nominal dimensions 200×200×152 mm (8×8×6 in.) were used in this study. The typical specimen dimensions with strengthening system are illustrated in **Fig. 1**.

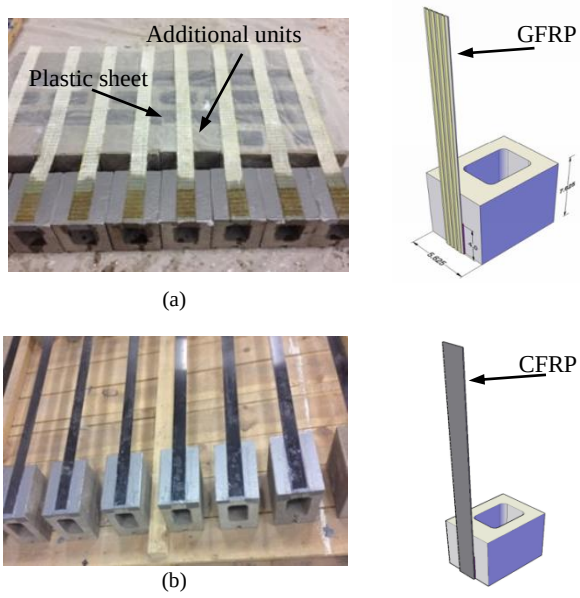

Fig. 1. Typical specimen dimensions with different types of fiber (a) GFRP (b) CFRP

The experimental work presented in this paper consisted of two groups. The first group focused on bond behavior when the EB-FRP was subjected to tension force simultaneously with applying temperature. The second group investigated the performance of strengthened units exposed to the 150 cycles of heating at 50 °C (122 °F) and cooling at -18 °C (0 °F) then the specimens tested later after exposure, which represents the traditional durability exposure test procedure.

Table 1 provides an overview of the types of fibers, adhesive material, FRP width and temperature when applying load for phase one.

The specimens were designated with three parts. The first part represents the type of fiber (GFRP sheet vs CFRP laminate). The second part identifies the type of adhesive: namely "T" for Tyfo S epoxy, "S" for SikaDur 30 epoxy. The third part refers to the temperature at the test. The character "A" refers to ambient temperature while "C" represents cycles of different temperature. As an example, the code GFRP-T-C refers to a specimen strengthened by GFRP sheet using Tyfo S epoxy and tested after applying cycles of different temperature.

Table 1. Experimental test matrix.

Wall	Specimen ID	Type of fiber	Sheet width (in.)	Adhesive material
1	GFRP-T-A	Glass	2	Tyfo S
2	GFRP-T-120	Glass	2	Tyfo S
3	GFRP-T-0	Glass	2	Tyfo S
4	GFRP-T-C	Glass	2	Tyfo S
5	CFRP-S-A	Carbon	2	SikaDur 30
6	CFRP-S-120	Carbon	2	SikaDur 30
7	CFRP-S-0	Carbon	2	SikaDur 30
8	CFRP-S-C	Carbon	2	SikaDur 30

Note: 1.0 mm=0.039 in., T (°C) = [T (°F) – 32] × 5/9

Strengthening materials and characterizations

The FRP composite materials consisted of fibers to provide the main reinforcing element to resist the applied load and the resin to hold and protect the fibers. The components of FRP composite system are developed as one package. In this study, the components of composite system are used based on manufacture recommendation.

The strengthening system (Tyfo SEH-51A) is a composite system that composed of glass fabric combined with Tyfo S Epoxy resins.

The EB technique for GFRP sheet consisted of SEH glass fabric and Tyfo S epoxy. The Tyfo S epoxy matrix is an ambient cure adhesive composed of two components. Tyfo SEH-51 is unidirectional glass fabric oriented at 0° direction with additional glass cross fiber at 90° to hold the main fabric together.

The second strengthening system used in this study is pre-cured CFRP laminate with SikaDur 30 epoxy resin. The CFRP laminate was made of 60% by volume of fibers embedded into epoxy resin under a pultrusion process. The SikaDur30 is a high modulus, high strength, structural epoxy resin used for bonding FRP externally to concrete, masonry, steel, etc.

According to the ASTM D3039-14, the minimum ultimate tensile strength and tensile modulus for the glass fiber composite in primary direction of Tyfo SHE-51 composite were 575 MPa (83 ksi) and 26.1 GPa (3785 ksi) respectively. One layer of glass fiber composite with 1.3 mm (0.05 in.) thickness has an elongation at break of 2.1%.

Based on ASTM D3039-14, the guaranteed tensile strength of CFRP is reported by the manufacturer to be 2400 MPa (350 ksi), with a tensile modulus of elasticity of 131 GPa (19000 ksi). The CFRP laminate with 1.4 mm (0.055 in.) thickness has an ultimate strain of 1.7% at failure.

The Tyfo S epoxy mixed at a volume ratio of 100:42 (resin: hardener) has a manufacturer properties for ultimate tensile strength and maximum strain were 72.4 MPa (10490 psi) and 5%, respectively. SikaDur 30, an adhesive bonding material that is a mixture of two parts, resin (A) and hardener (B) was mixed at a volume ratio of 100:30 to bind CFRP laminate. Based on ASTM D638-14 [13], the tensile strength and elongation at break provided by the manufacturer were 24.8 MPa (3600 psi) and 1%, respectively.

The average compressive strength of a masonry unit at test age was found to be 21 MPa (3,000 psi).

Specimen design

The single-shear pull test consisted of a masonry unit bonded with an FRP sheet or laminate. The advanced composite is located at the plane of symmetry of the concrete masonry unit. The total length of fiber sheet was 840 mm (33 in.), and the bonded length was 100 mm (4 in.), where 12 mm (0.5 in.) was left for the bottom of the specimen to monitor the fiber slip failure. The sheet and laminate width was 50 mm (2 in.). The free end of the fiber was attached to steel plates bolted together with four bolts to enable uniform load application without damage or slippage of gripped fiber. To ensure specific bonded length, duct tape was used as a bond breaker for a length of 90 mm (3.5 in.) from the top of the specimen. The description of the strengthened specimens is illustrated in **Fig. 1**.

Installation of advanced composite

The first step in the strengthening procedure was surface preparation to create optimal bond between FRP and substrate. The surface preparation included placing the masonry unit inside the oven to ensure complete drying of the surface, manually cleaning the surface using a wire brush and vacuuming to remove the residual dust resulting from wire brushing. The levelled and dried surface should be adopted to prevent premature peeling of FRP resulting from an uneven surface. For specimens strengthened with GFRP, Tyfo S epoxy resin was applied to serve as a prime filler layer to prepare the surface before installation of the GFRP sheet. The wet lay-up procedure was used to bond GFRP on the masonry prepared surface. The pre-cut SEH51 fabric was saturated with Tyfo S epoxy resin before it was applied to the masonry substrate to provide good bonding. Additional masonry units were used in the same line of the strengthened unit to ensure level and straight fabric as shown in **Fig.1**. The fabric was aligned, and the air bubbles were removed at the interface using

a hand roller until the fabric was fully attached to the substrate. The surface of additional units was covered by plastic sheet to avoid adherence with GFRP sheet.

Temperature and surface moisture of masonry unit at the time of applying advanced composite are the essential parameters that affect the strengthening procedure and the behavior of the strengthening system. The epoxy was applied at room temperature 21°C (70 °F), which satisfies the manufacturer's temperature installation limits. The specimens were kept at the lab temperature for one day then each plastic sheet was peeled off. The curing period for Tyfo S epoxy resin was three days at 60 °C (140 °F).

SikaDur 30 adhesive was used to bond the Aslan 400 CFRP laminate. Before applying SikaDur 30, the roughened face of CFRP laminate was wiped with solvent for cleaning to improve the bonding. The FRP sheet or laminate was bonded to the masonry specimen so that the fiber was in the direction of the load path. All the strengthened specimens were cured for one week prior to testing.

Test setup

A steel frame for single-lap shear test was carefully fabricated to carry out the experimental test for specimens subjected to direct temperature or cycles of heating and cooling. The masonry specimen was restrained against vertical movement during the test by bolting steel frame to the testing machine base. A thick steel plate was inserted between the frame and the top of the specimen to ensure uniform distributed pressure over the restrained specimen.

For the specimens subjected to direct temperature, the steel frame was positioned inside a chamber with dimensions 300mm x 600mm x 800mm (12in. x 24in. x 32in.), as shown in **Fig. 2 (a)**. The maximum temperature capacity of the chamber is 100 °C (212 °F), while the minimum temperature is -70 °C (-94 °F). To minimize the time of the test, the specimens were pre-conditioned to reach thermal equilibrium using an oven or refrigerator. The specimens were heated in the oven or cooled in the refrigerator and then moved to the chamber. The chamber was installed around the MTS universal testing machine with a 250 kN (56.2 kip.) capacity.

Loading rate and instrumentation

The load was applied in displacement control at a rate of 0.25 mm/min (0.01 in./min) through an MTS computer control station up to the load peak value. The global slip was measured between the fiber and the top of the specimen using high temperature linear variable displacement transducers (LVDTs). In addition, strain gauges were installed on three locations of bonded length at 25 mm (1in.), 50 mm (2in.), and 75mm (3in.) from the bottom of the bonded length. Four type-K thermocouples with diameter of 1.2mm (0.047in.) were fixed at different locations. Temperature on tested specimens was measured from four thermocouples placed 1) inside the core of the concrete block unit, 2) outside the surface of the concrete block unit, 3) at the adhesive layer, and 4) at the fiber of different strengthening systems. The locations of thermocouples are illustrated in **Fig. 2 (b)**. All the wires were connected to the data acquisition system outside the environmental chamber.

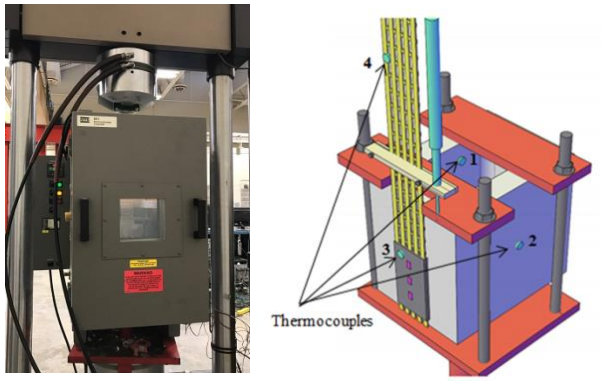

(a) (b)

Fig. 2. Test setup (a) heating and cooling chamber, (b) locations of thermocouples.

Test procedure for specimens under direct temperature

The specimens in this phase of study were heated up to 49 °C (120 °F) in a furnace or cooled down to -18°C (0 °F) in a refrigerator, and then the specimens were brought to the chamber that was attached to the MTS universal testing machine to ensure that the specimens were at temporal with desired temperature. The specimens were loaded when the readings of four thermocouples were close enough as shown in **Fig. 3 (a)**.

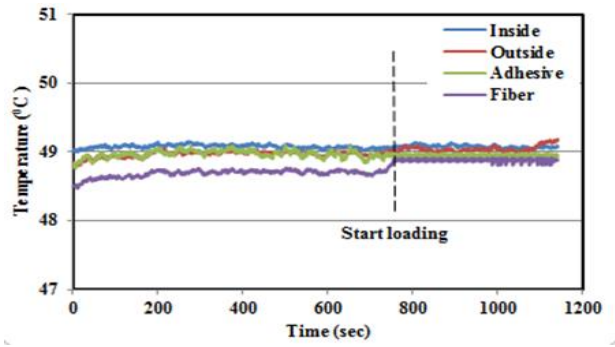

(a)

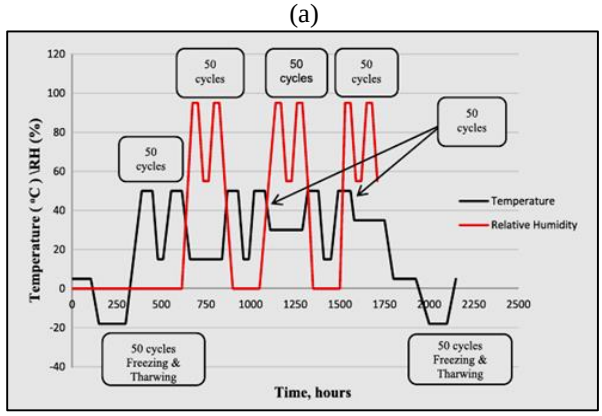

(b)

Fig. 3. Applied temperature (a) Time- temperature curve obtained from the four thermocouples, (b) cycles of temperature exposure regime.

Test procedure for specimens exposed to cyclic temperature

The specimens in this phase of study were subjected to the conventional heating and freezing cycles in the environmental chamber as follows:

- Freeze-thaw cycles: 100 freeze and thaw cycles were applied on strengthened specimens. Each freeze-thaw cycle consisted of freezing at -17.8°C (0°F) for 50 minutes and thawing at 4.4°C (40°F) for 50 minutes. The transition period between freezing and thawing was 30 minutes.
- High temperature cycles: 150 alternating cycles of extreme temperature from 27 to 50°C (80 to 120°F) were used. An extreme temperature cycle consisted of temperature variation between 27 °C (80 °F) for 25 minutes and 50 °C (120 °F) for 25 minutes. The transition period between high and low temperature was 20 minutes.

The exposure regime of heating and cooling for specimens in the environmental chamber is shown in **Fig. 3 (b)**. All the specimens were subjected to an identical heating and cooling rate to ensure the consistency of the temperature during the loading process. After exposure, the bond behavior investigated by testing the specimens using steel frame under an ambient temperature.

Table 2. The average test results.

Wall	Specimen ID	Max. load P_u (kN)	Max. Strain (mm/mm)	Mode of failure*
1	GFRP-T-A	15.56	0.00790	D-A/M
2	GFRP-T-120	6.45	0.00324	S-F/E
3	GFRP-T-0	16.69	0.00842	D-A/M
4	GFRP-T-C	13.15	0.00750	T-R
5	CFRP-S-A	23.56	0.00124	D-A/M
6	CFRP-S-120	13.8	0.00127	S-F/E
7	CFRP-S-0	23.51	0.00120	D-SL
8	CFRP-S-C	22.24	0.00118	D-A/M

* D-A/M: debonding at adhesive-masonry interface, D-SL: debonding due to shearing in laminate, D-F/E: debonding at fiber- epoxy interface, T-R tensile rupture of the advanced composite, and S-F/E: slipping at fiber- epoxy interface.

Results and discussion

The summary of the maximum pull-out load (P_u), mid-bonded length strain at maximum force (ε_u), and the mode of failure for all specimens are reported in **Table 2**. This table represents the average test results obtained from two identical specimens for each case. It was observed that the maximum pull-out load significantly decreased at 48°C (120°F) by an average 50% for specimens strengthened with GFRP or CFRP. On the other hand, there is no discernible negative effect of -18°C (0°F) on the performance of advanced composite when compared to the performance at ambient temperature. The reduction in the ultimate pull-out force for high temperature specimens was due to degradation of the epoxy adhesive. The bond degradation of specimens strengthened with GFRP subjected to cycles of heating and cooling temperature was higher than the bond degradation of specimens strengthened with CFRP.

Pull-out force-global slip relationship

For specimens subjected to either direct temperature or cycles of heating and cooling temperature, two samples were considered per each case. The average maximum pull-out force was 23.56kN (5.3 kip.). The relationships between pull-out force and global slip of representative specimens are shown in **Fig. 4**.

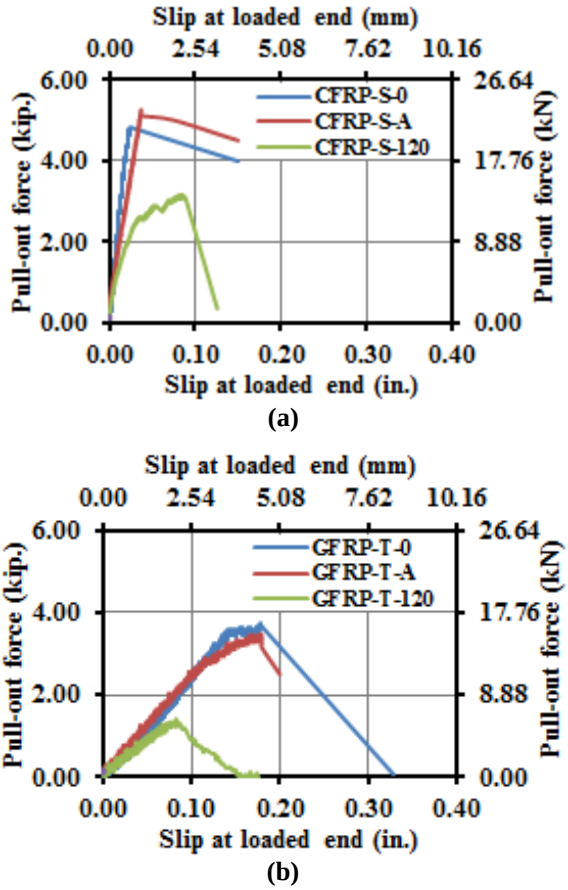

Fig. 4. Pull-out force vs. global slip relationship for (a) EB-CFRP, (b) EB-GFRP

The specimens were grouped based on the types of fibers. For both types, the pull-out force vs global slip curves were characterized by a linear relationship up to the ultimate load, and then the capacity dropped suddenly due to debonding as a result of concrete or epoxy cover splitting. The heated specimens exhibited a gradual failure due to softening of the (concrete-resin) interface up to failure, as shown in **Fig. 4 (a and b)**.

The key factor for load transfer mechanism is the bond between the strengthening system and the substrate. The debonding surface for specimens subjected to ambient or low temperature was either fiber-epoxy surface or epoxy-substrate surface. For the same specimens subjected to high temperature, the bond was totally lost due to adhesive softening.

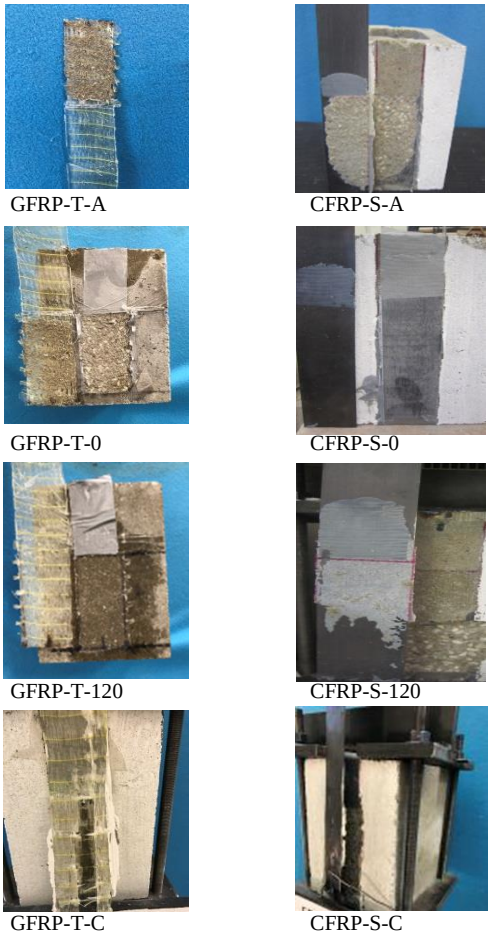

Fig. 4. Modes of failure for different temperatures.

Modes of failure

All modes of failure are illustrated in **Fig. 4**. In general, the result of this study showed that the debonding from the masonry unit is the most common failure mode for specimens subjected to ambient temperature. For those specimens, the debonding surface was at adhesive-masonry interface in which a thin layer of masonry face shell was attached to the FRP sheet or laminate after failure.

For specimens strengthened with GFRP and subjected to low temperature, the mode of failure was almost the same comparing with the same specimen subjected to ambient temperature but little layer of masonry was attached to the FRP sheet. Debonding due to shearing in laminate occurred for specimen strengthened with CFRP laminate and subjected to low temperature.

For specimens subjected to high temperature, an adhesive failure was observed. Slipping at fiber- epoxy interface occurred due to softening of the adhesive layer.

Cycles of heating and cooling led to tensile rupture of the advanced composite (GFRP specimen) or debonding due to adhesive splitting (CFRP specimen). The change in mode of failure in this phase occurred due to adhesive microcracks that generated as a result of heating/cooling cycles.

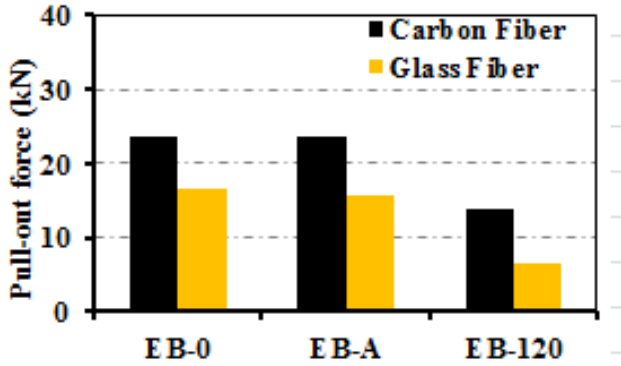

Fig. 5. Effect of temperature on advanced composite

Effect of different temperatures

The effects of temperature on different types of advanced composite are more evident by looking at the column charts in **Fig. 5**.

The decrease of the ultimate pull-out force can be observed for temperatures close to the heat distortion temperature (HDT). In particular, ultimate pull-out force was decreased compared to ultimate pull-out force of the same specimens at ambient temperature due to degradation in adhesive material. The ultimate capacity was decreased by 59% in the case of specimens strengthened with EB-GFRP sheets, and 42% for specimens strengthened with CFRP-EB laminate. The reduction in pull-out force capacity is due to dramatic reduction of FRP bond to the substrate. The temperature affected the mode of failure by changing from a mixed cohesive-adhesive with concrete detached to a fully adhesive failure at elevated temperature. The pull-out force for specimens strengthened with GFRP were less than the capacity of specimens strengthened with CFRP due to high temperature resistance for pre-cured CFRP laminate compared to wet-layup GFRP sheets.

Effect of cycles of heating and cooling

The average maximum pull-out force was 22.24 kN (5.0 kip). The pull-out force vs. global slip curve for specimens strengthened with different types of fibers is shown in **Fig. 6**.

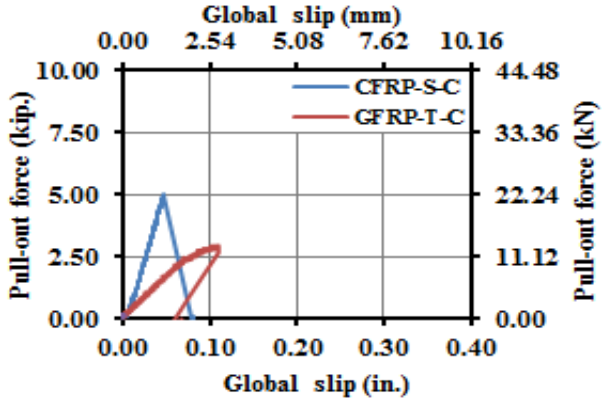

Fig. 6. Effect of exposure condition on advanced composite

For the specimens exposed to cycles of heating followed by cooling, microcracks that generated in adhesive material affected the mode of failure which transitioned from a debonding (due to masonry face shell splitting) to a debonding due to epoxy splitting.

In order to compare between the specimens strengthened with different types of fibers in the second phase (subjected to cyclic temperature), an effectivity index was considered. The effectivity index represents the ratio between the ultimate pull-out force for specimen subjected to cycles of heating and cooling to the same specimen subjected to ambient temperature ($P_u/P_{u,A}$). The effectivity index for specimen strengthened with EB GFRP was 85%, which is less than the effectivity index of EB CFRP (94%). This performance was attributed to the excellent quality control of the manufactured CFRP laminate compared to GFRP wet-layup. The reduction of pull-out capacity due to the cyclic exposure to the temperatures close to the HDT of the epoxy adhesive was insignificant due to the reset process of epoxy prior to the bond test.

Conclusion

This paper presents a study on bond behavior under direct load and service temperature. Based on this research, the following conclusions can be drawn:

1. The relationship of pull-out force and global slip was linear up to ultimate and then the capacity dropped either suddenly due to complete debonding (in case of low and ambient temperature) or gradually due to softening of the masonry-resin interface (in the case of high temperature).
2. Debonding mode of failure was identified from this study as follows: debonding due to masonry face shell or epoxy cover splitting, debonding due to shearing in laminate, debonding at the adhesive-masonry interface, debonding at the fiber-epoxy interface, tensile rupture of the advanced composite and slipping at the fiber-epoxy interface.
3. The FRP-epoxy bond properties reduced up to 59% when exposed to high service temperatures. This reduction was attributed to the rapid deterioration of the epoxy-substrate adhesion when the temperature is close to or exceeds the heat distortion temperature (HDT) of the epoxy.
4. The pull-out force for specimens strengthened with GFRP was less than the capacity of specimens strengthened with CFRP due to high temperature resistance for pre-cured CFRP laminate compared to wet-layup GFRP sheets.
5. For EB strengthening systems exposed to cycles of heating and cooling, microcracks generated in adhesive material changed the mode of failure from debonding due to masonry face shell splitting to debonding due to epoxy splitting associated with pull-out force reduction by 10%.

Acknowledgements

The authors wish to acknowledge the support of Midwest Block & Brick in Jefferson City, Missouri and Hughes Brothers in Seward, Nebraska. The authors also wish to thank the technical support staff in not only the Department of Civil and Environmental Engineering and also the Center for Infrastructure Engineering Studies (CIES) at Missouri University of Science and Technology for their efforts in this research study. Any opinions, findings, conclusions, and recommendations presented in this paper are those of the authors and do not necessarily reflect the views of the sponsor or supporting agencies.

Author's contributions

Conceived the plan: Z. Al-Jaberi and J.J. Myers; Performed the expeirments: Z. Al-Jaberi and J.J. Myers; Data analysis: Z. Al-Jaberi and J.J. Myers; Wrote the paper: Z. Al-Jaberi, J.J. Myers, K. Chandrashekhara (ZA, JM, KC are the initials of authors). Authors have no competing financial interests.

References

1. Tumialan, J.G., F. Micelli, and A. Nanni, Strengthening of masonry structures with FRP composites, in Structures 2001: A Structural Engineering Odyssey. 2001. p. 1-8.
2. Al-Jaberi, Z., J.J. Myers, and M.A. ElGawady, Pseudo-static cyclic loading comparison of reinforced masonry walls strengthened with FRCM or NSM FRP. Construction and Building Materials, 2018. 167: p. 482-495.
3. Al-Jaberi, Z., J. Myers, and M. ElGawady, Flexural capacity of out-of-plane reinforced masonry walls strengthened with externally bonded(EB) FRP, in 7th International Conference on Advanced Composite Materials in Bridges and Structures 2016: Vancouver, British Columbia, Canada
4. Tatar, J. and H. Hamilton, Bond durability factor for externally bonded CFRP systems in concrete structures. Journal of Composites for Construction, 2015. 20(1): p. 04015027.
5. Masia, M.J., et al., Behaviour of NSM FRP masonry bond under elevated temperatures. Proceedings of the Institution of Civil Engineers-Construction Materials, 2015. 169(1): p. 27-38.
6. Stratford, T. and L. Bisby, Effect of warm temperatures on externally bonded FRP strengthening. Journal of Composites for Construction, 2011. 16(3): p. 235-244.
7. Li, K., et al., Bond–Slip Relationship for CFRP Sheets Externally Bonded to Concrete under Cyclic Loading. Materials, 2018. 11(3): p. 336.
8. Chowdhury, E., et al., Mechanical characterization of fibre reinforced polymers materials at high temperature. Fire technology, 2011. 47(4): p. 1063-1080.
9. Leone, M., S. Matthys, and M.A. Aiello, Effect of elevated service temperature on bond between FRP EBR systems and concrete. Composites Part B: Engineering, 2009. 40(1): p. 85-93.
10. Burke, P.J., L.A. Bisby, and M.F. Green, Effects of elevated temperature on near surface mounted and externally bonded FRP strengthening systems for concrete. Cement and Concrete Composites, 2013. 35(1): p. 190-199.
11. Cromwell, J., K. Harries, and B. Shahrooz, Environmental durability of externally bonded FRP materials intended for repair of concrete structures. Construction and Building Materials, 2011. 25(5): p. 2528-2539.
12. Maljaee, H., et al., FRP–brick masonry bond degradation under hygrothermal conditions. Composite Structures, 2016. 147: p. 143-154.
13. ASTM.(2014). Standard Test Method for Tensile Properties of Plastics1 ASTM D638-14. 2014. West Conshohocken, PA.

